International Journal of Fracture 64: 239–249, 1993.

Effect of curvature at the crack tip on the stress intensity factor for curved cracks

NAO-AKI NODA and KAZUHIRO ODA
Department of Mechanical Engineering, Kyushu Institute of Technology, 1-1 Sensuicho, Tobataku, Kitakyushu 804, Japan

Received 29 January 1993; accepted 13 September 1993

Abstract. In this paper, the numerical solution of the hypersingular integral equation using the body force method in curved crack problems is presented. In the body force method, the stress fields induced by two kinds of standard set of force doublets are used as fundamental solutions. Then, the problem is formulated as a system of integral equations with the singularity of the form r^{-2}. In the numerical calculation, two kinds of unknown functions are approximated by the products of the fundamental density functions and power series. The calculation shows that the present method gives rapidly converging numerical results for curved cracks under various geometrical conditions. In addition, a method of evaluation of the stress intensity factors for arbitrary shaped curved cracks is proposed using the approximate replacement to a simple straight crack.

1. Introduction

In the investigation of fatigue crack growth behavior based on linear fracture mechanics, it is quite important to calculate exactly the stress intensity factor of the crack for various geometric configurations. In the two-dimensional curved crack problem, the solution for a circular-arc crack in an infinite plate has been first presented by Sih-Paris-Erdogan [1] using the stress function given by Muskhelishvili [2]; however, Atluri-Kobayashi-Nakagaki [3] and Cotterell-Rice [4] have corrected the error of the expression of the solution. Ioakimidis and Theocaris [5] have given the numerical solutions of a circular-arc crack in an isotropic elastic half-plane. Chen et al. [6] have analyzed crack problems of parabolic shape, sine shape and snake shape in an infinite plate. Other curved crack problems have been analyzed by an approximate method using the first order solution [4, 7] and using the solution of the circular-arc crack [8, 9]. However, little attention has been given to the relation between curvature at the tip of the curved crack and the stress intensity factor.

In the previous papers [10, 11], numerical solution of the singular integral equation of the body force method has been discussed and the various crack problems have been shown to be solved with higher accuracy compared with previous research. In this study, the method is applied to the analysis of the curved crack problem. As a basic model, the problem of a crack that consists of a straight part and a circular-arc part is treated. The calculation is carried out for the curved crack under various geometrical conditions in order to investigate the effect of curvature at the crack tip on the stress intensity factor. In addition, a method of evaluation of the stress intensity factors for arbitrary shaped curved cracks is proposed using the approximate replacement to a simple straight crack.

2. Numerical solution of the singular integral equation

In this section, by taking as an example the tension of a semi-infinite plate with a circular-arc edge crack (Fig. 1), a method of solution will be explained. The hypersingular integral equation

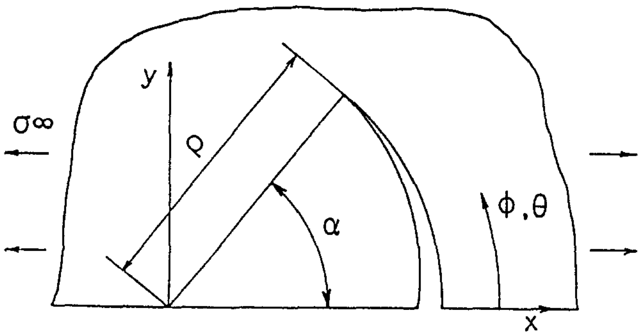

Fig. 1. Circular-arc edge crack in a semi-infinite plate under uniform tension.

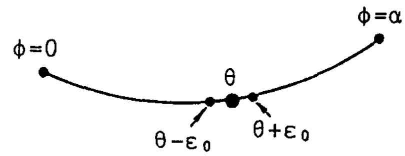

Fig. 2. Division of the integration interval.

for this problem can be formulated by means of the body force method [11, 15]. This method uses the stress field induced by two kinds of standard set of force doublets in an infinite plate as a fundamental solution. The problem is reduced to the following integral equation, where the densities of the body force doublets (continuously distributed pairs of point forces) along the imaginary boundary of the crack, tension and shear type $f_1(\phi)$ and $f_2(\phi)$, are to be unknown functions

$$\fint_0^\alpha h_{11}(\theta,\phi) f_1(\phi)\,\mathrm{d}\phi + \int_0^\alpha H_{11}(\theta,\phi) f_1(\phi)\,\mathrm{d}\phi + \fint_0^\alpha h_{12}(\theta,\phi) f_2(\phi)\,\mathrm{d}\phi$$

$$+ \int_0^\alpha H_{12}(\theta,\phi) f_2(\phi)\,\mathrm{d}\phi = -\sigma^\infty \cos^2\theta, \tag{1a}$$

$$\fint_0^\alpha h_{21}(\theta,\phi) f_1(\phi)\,\mathrm{d}\phi + \int_0^\alpha H_{21}(\theta,\phi) f_1(\phi)\,\mathrm{d}\phi + \fint_0^\alpha h_{22}(\theta,\phi) f_2(\phi)\,\mathrm{d}\phi$$

$$+ \int_0^\alpha H_{22}(\theta,\phi) f_2(\phi)\,\mathrm{d}\phi = \sigma^\infty \sin\theta\cos\theta. \tag{1b}$$

Equation (1) is virtually the boundary conditions on the imaginary boundary; that is, $\sigma_n = 0$, $\tau_{nt} = 0$. Here $h_{ij}(\theta, \phi)$ $(i, j = 1, 2)$ is stresses due to the standard set of force doublets in an infinite plate and $H_{ij}(\theta, \phi)$ is the function known to satisfy the boundary condition expected at the crack surface.

In the numerical solution of (1), the unknown function $f_i(\phi)$ $(i = 1, 2)$ is approximated by the product of the fundamental density function $w_i(\phi)$ and the power series ϕ^n

$$f_1(\phi) = F_{\mathrm{I}}(\phi) w_1(\phi), \quad F_{\mathrm{I}}(\phi) \cong \sum_{n=0}^{N-1} a_n \phi^n, \quad w_1(\phi) = \frac{(\kappa+1)^2 \sigma^\infty}{2(\kappa-1)} \rho\sqrt{\alpha^2 - \phi^2}, \tag{2a}$$

$$f_2(\phi) = F_{\mathrm{II}}(\phi) w_2(\phi), \quad F_{\mathrm{II}}(\phi) \cong \sum_{n=0}^{N-1} b_n \phi^n, \quad w_2(\phi) = \frac{(\kappa+1)\sigma^\infty}{2} \rho\sqrt{\alpha^2 - \phi^2}, \tag{2b}$$

where N is a number of collocation points, $\kappa = 3 - 4\nu$ in plane strain, and ν is Poisson's ratio.

Using the approximation method mentioned above, the problem is reduced to determining the coefficients a_n and b_n in (2). The convenient set of collocation points is given by

$$\theta_j = \tfrac{1}{2}\alpha \cos\left(\frac{2j-1}{N}\frac{\pi}{2}\right) + \tfrac{1}{2}\alpha, \quad (j = 1, 2, \dots, N). \tag{3}$$

The stress intensity factor can be calculated from

$$K_{\mathrm{I,II}} = F_{\mathrm{I,II}}(\alpha)\sigma^{\infty}\sqrt{\pi\rho\alpha}. \tag{4}$$

The present method in this section can be applied to various curved crack problems. As an example, a crack that consists of a straight part and a circular-arc part is considered in this study. The boundary conditions along the straight part of the crack are satisfied by the product of the fundamental density functions and Chebyshev polynomials as shown in [10, 11].

3. Evaluation of singular integral

The integration of the first and the third terms in the left-hand sides of (1) involve singular terms. In the analysis of straight crack problems, the singular integral is easily evaluated by the formula using Chebyshev polynomials [10–13]. However, in the curved crack problem, the formula is not available; therefore, the following method of evaluation of finite-part integrals is applied [15].

The integration interval is divided into three parts as shown in Fig. 2.

$$I = \int\!\!\!\!\!\!=_{0}^{\alpha} h(\theta, \phi) f(\phi)\,\mathrm{d}\phi$$

$$= \int_{0}^{\theta-\varepsilon_0} h(\theta, \phi) f(\phi)\,\mathrm{d}\phi + \int\!\!\!\!\!\!=_{\theta-\varepsilon_0}^{\theta+\varepsilon_0} h(\theta, \phi) f(\phi)\,\mathrm{d}\phi + \int_{\theta+\varepsilon_0}^{\alpha} h(\theta, \phi) f(\phi)\,\mathrm{d}\phi = I_1 + I_2 + I_3. \tag{5}$$

The first and the third integral can be easily evaluated by the numerical integration procedure. The second integral can be expressed as follows by letting $\phi = \theta + \varepsilon$

$$I_2 = \int\!\!\!\!\!\!=_{-\varepsilon_0}^{\varepsilon_0} h(\theta, \theta+\varepsilon) f(\theta+\varepsilon)\,\mathrm{d}\varepsilon = \int\!\!\!\!\!\!=_{-\varepsilon_0}^{\varepsilon_0} \left(\frac{c_1}{\varepsilon^2} + \frac{c_2}{\varepsilon} + c_3 + \cdots\right)\mathrm{d}\varepsilon. \tag{6}$$

The first term integral in the right-hand side in (6) is evaluated as the meaning of the finite-part integral proposed by Hadamard [14]. The second term integral, which is interpreted as meaning Cauchy's principle value, should be zero. Neglecting the terms of a higher order than ε_0^2, we find

$$I_2 \cong -\frac{2c_1}{\varepsilon_0} + 2c_3\varepsilon_0. \tag{7}$$

Then the singular integrals are calculated by determining of the coefficients c_1 and c_3 in (6).

4. Numerical results and discussion

4.1. Circular-arc crack in an infinite plate

Since the exact solution for a circular-arc crack in an infinite plate is available, the accuracy of the result obtained by the present method is verified through the comparison with the exact solution. Table 1 shows the stress intensity factors calculated by the previous body force method, in which the unknown functions are approximated by the stepped function instead of the power series in (2). Here N is the number of collocation points and the symbol ∞ (100–150) designates the extrapolated value using the results of $N = 100$ and 150 on the basis of the linear relationship between the SIF and $1/N$. As shown in Table 1, the results obtained by the previous method using stepped function coincide with the exact solution in the 3 digits.

On the other hand, Table 2 shows the results obtained by the present method. The present results coincide with the exact solution in the 7 digits completely when $N = 6$. It is found that the present method gives rapidly converging numerical result with short CPU time.

4.2. Curved crack in an infinite plate

To investigate the effect of curvature at the crack tip on the stress intensity factor, a curved crack that consists of a straight part and a circular-arc part is considered as a basic crack model. In Table 3, dimensionless SIFs at the crack tip B for various values of the relative curvature $\rho/2c$ and the angle α are shown, where $2c$ is the projected length of the total crack in a direction perpendicular to the tensile axis. In consideration of the estimation of the SIF for an arbitrary shaped crack in an actual structure, the present results are compared with the SIF of the straight crack with the same inclination angle α and with the same projected length $2c$ as shown in Fig. 3. As shown in Table 3, the value of F_{I} at the tip B of the curved crack can be estimated by that of the straight crack within about 4 percent when $\rho/2c > 0.2$ and $\alpha < 45°$. On the other hand, the difference of the values of F_{II} between the curved and the straight crack is quite large.

Next, the effect of the position of crack tip A on the SIF at the crack tip B is considered. The position of crack tip A varies in the range that $-15° \leqslant \beta \leqslant 45°$ as shown by the parameter β in Fig. 4. The results are shown in Table 4, when $\rho/2c = 0.2 \sim 0.8$ and $\alpha = 30°$. It is seen that the SIF at crack tip B is not much influenced by the position of the other crack tip A, if $\rho/2c > 0.4$. Judging from Table 3 and 4, the mode I SIF of arbitrary curved crack can be approximately evaluated by that of the straight crack with the same inclination angle and with the same projected length of the curved crack, when $\rho/2c > 0.4$ and $\alpha < 45°$.

4.3. Circular-arc edge crack in a semi-infinite plate

The circular-arc edge crack in a semi-infinite plate under uniform tension is considered. In the case that the tangent of the crack tip is perpendicular to the half-plane boundary, the dimensionless SIFs for various values of θ obtained by the present analysis are shown to be compared with the results of Ioakimidis et al. [5] in Table 5. Both results are in good agreement with each other. In Table 5, F_{I}^* is the dimensionless SIF based on $\sigma^{\infty}\sqrt{\pi b}$, where $b = \rho \sin \alpha$ is the projected crack length. The values of F_{I}^* are in close agreement with the well-known value 1.1215. The corresponding values of F_{II} can be seen almost to vanish.

Table 1. Convergency of the SIF for circular-arc crack obtained by using the stepped function ($k_{I,II} = K_{I,II}/\sigma^{\infty}\sqrt{\rho}$)

N	$\alpha = 30.0,\ \beta = 0.0$		$\alpha = 30.0,\ \beta = 30.0$			
	$k_{IA,B}$	$k_{IIA,B}$	k_{IA}	k_{IIA}	k_{IB}	k_{IIB}
30	0.97846	0.57695	1.1603	0.058016	0.38559	0.78451
50	0.97650	0.58114	1.1620	0.053928	0.38177	0.78581
80	0.97559	0.58322	1.1630	0.051956	0.37990	0.78652
100	0.97534	0.58386	1.1632	0.051378	0.37935	0.78675
150	0.97506	0.58463	1.1636	0.050697	0.37869	0.78706
200	0.97495	0.58497	1.1638	0.050409	0.37840	0.78722
∞(100–150)	0.97450	0.58517	1.1644	0.049336	0.37736	0.78769
∞(150–200)	0.97463	0.58601	1.1644	0.049543	0.37754	0.78768
Exact	0.97496	0.58562	1.1643	0.050048	0.37797	0.78768

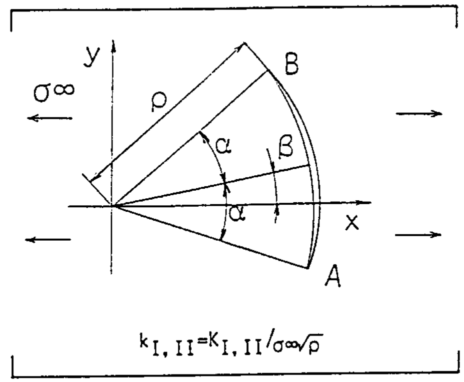

Table 2. Convergency of the SIF for circular-arc crack obtained by using the power series ($k_{I,II} = K_{I,II}/\sigma^{\infty}\sqrt{\rho}$)

N	$\alpha = 30.0,\ \beta = 0.0$		$\alpha = 30.0,\ \beta = 30.0$			
	$k_{IA,B}$	$k_{IIA,B}$	k_{IA}	k_{IIA}	k_{IB}	k_{IIB}
2	0.9895561	0.5619829	1.151651	0.05946876	0.4074583	0.7688413
4	0.9749634	0.5856141	1.164283	0.05005156	0.3779830	0.7876736
6	0.9749593	0.5856211	1.164287	0.05004821	0.3779741	0.7876775
8	0.9749593	0.5856211	1.164287	0.05004820	0.3779741	0.7876775
10	0.9749593	0.5856212	1.164287	0.05004821	0.3779741	0.7876775
Exact	0.9749593	0.5856211	1.164287	0.05004821	0.3779741	0.7876775

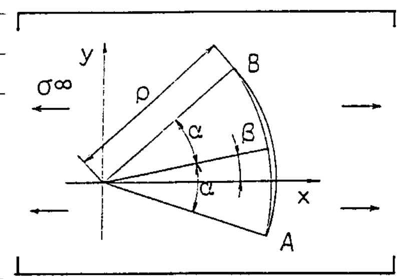

Table 3. Dimensionless SIF of a crack that consists of a straight part and circular-arc part ($F_{I,II} = K_{I,II}/\sigma^{\infty}\sqrt{\pi c}$)

$\rho/2c$ \ α	15.0		30.0		45.0		60.0	
	F_I	F_{II}	F_I	F_{II}	F_I	F_{II}	F_I	F_{II}
0.1	0.9656	0.1616	0.8547	0.3257	0.6746	0.4571	0.4480	0.5327
0.2	0.9623	0.1741	0.8389	0.3557	0.6387	0.5006	0.3890	0.5820
0.4	0.9581	0.1907	0.8207	0.3934	0.6009	0.5532	0.3338	0.6386
0.6	0.9554	0.2024	0.8100	0.4183	0.5826	0.5847	0.3141	0.6675
0.8	0.9533	0.2116	0.8034	0.4361	0.5742	0.6042	0.3110	0.6797
1.0	0.9517	0.2190	0.7992	0.4492	0.5718	0.6152	0.3165	0.6805
Straight	0.9493	0.2544	0.8059	0.4653	0.5946	0.5946	0.3536	0.6124

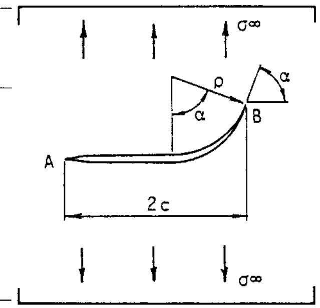

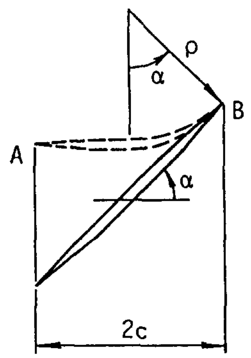

Fig. 3. Estimation of the SIF using the approximate replacement to a straight crack.

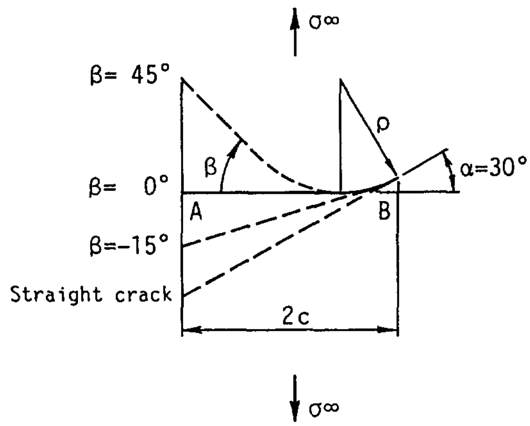

Fig. 4. Effect of the position of the crack tip A on the SIF at the crack tip B.

Table 4. Values of F_{I} and F_{II} in Fig. 4

$\rho/2c$	0.2		0.4		0.6		0.8	
β	F_{I}	F_{II}	F_{I}	F_{II}	F_{I}	F_{II}	F_{I}	F_{II}
−15.0	0.8165	0.4034	0.8130	0.4172	0.8107	0.4267	0.8091	0.4340
0.0	0.8389	0.3557	0.8207	0.3934	0.8100	0.4183	0.8034	0.4361
15.0	0.8642	0.3188	0.8228	0.3780	0.8005	0.4175	0.7891	0.4446
30.0	0.8965	0.2832	0.8301	0.3559	0.7934	0.4103	0.7777	0.4478
45.0	0.9448	0.2480	0.8597	0.3213	0.8003	0.3927	0.7749	0.4466
Straight	0.8059	0.4653	0.8059	0.4653	0.8059	0.4653	0.8059	0.4653

Table 5. Dimensionless SIF of the circular-arc edge crack, in which the tangent of the crack tip is perpendicular to the half-plane boundary ($F_{\mathrm{I}} = K_{\mathrm{I}}/\sigma^{\infty}\sqrt{\pi\rho\alpha}$, $F_{\mathrm{I}}^{*} = K_{\mathrm{I}}/\sigma^{\infty}\sqrt{\pi b}$, $b = \rho \sin \alpha$)

α	Present analysis		Ioakimidis et al. [5]
	F_{I}	(F_{I}^{*})	F_{I}
15.0	1.1152	(1.1216)	1.115
30.0	1.0962	(1.1218)	1.100
45.0	1.0647	(1.1221)	1.065
60.0	1.0206	(1.1223)	1.023
75.0	0.9642	(1.1224)	0.965

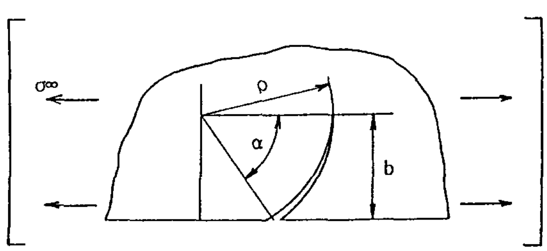

Next, the circular-arc edge crack as shown in Fig. 1 is analyzed. Table 6 shows the convergency of the SIFs. In the case of the edge crack problem, it is found that the convergency of the present results is extremely good. In Table 7, the dimensionless SIFs for various values of α are shown in comparison with the SIFs for an oblique edge crack. The angle of the oblique edge crack is chosen such as to have the same tangent of the tip of the circular-arc edge crack as shown in Fig. 5. As shown in Table 7, it can be seen that mode I SIFs of the straight crack conform more closely to one of the circular-arc cracks for a wide range of α. The values of F_{II} of the oblique edge crack are also in good agreement within 5 percent for $\alpha < 60°$.

4.4. Curved edge crack in a semi-infinite plate

Finally, the edge crack that consists of a straight part and a circular-arc part, which we called 'the curved edge crack' in this paper, is considered. The SIFs are calculated for various values of α and c_2/c_1, where α is the angle of the crack tip, c_1 is the projected crack length, and $c_2 = \rho \sin \alpha$ is the projected length of the circular-arc part. The dimensionless SIFs are shown in Table 8 in comparison with the SIFs for an oblique edge crack as shown in Section 4.3. As shown in Table 8, it can be seen that mode I SIFs of the straight crack are in close agreement with those of the curved edge crack for wide range of α and c_2/c_1. The difference between mode II SIFs for curved and straight edge crack is generally small except for the case of large α and small c_2/c_1.

In the case of the edge crack, it is found that the curvature of the crack tip does not have much effect on the stress intensity factor. Hence, the approximate SIF for arbitrary curved edge crack can be evaluated, if the inclined angle at the crack tip and the projected crack length are given.

In addition, the stress intensity normal to tensile directions is considered [16]. The edge crack subjected to uniform tension has a strong tendency to grow in a direction perpendicular to that of the applied stress and macroscopically the crack grows in that direction. At the crack tip, the stress σ_x on the y-axis as shown in Table 9 is expressed by

$$\sigma_x = \frac{\hat{K}_I}{\sqrt{2\pi y}} = \frac{\hat{F}_I \sigma^\infty \sqrt{\pi c_1}}{\sqrt{2\pi y}}, \tag{8}$$

$$\hat{K}_I = (\tfrac{3}{4}\cos\tfrac{1}{2}\alpha + \tfrac{1}{4}\cos\tfrac{1}{2}3\alpha)K_I + (\tfrac{3}{4}\sin\tfrac{1}{2}\alpha + \tfrac{3}{4}\sin\tfrac{1}{2}3\alpha)K_{II}. \tag{9}$$

Table 6. Convergency of the SIF for the circular-arc edge crack as shown in Fig. 1

N	$\alpha = 30.0$		$\alpha = 60.0$	
	F_I	F_{II}	F_I	F_{II}
4	0.920717	0.304933	0.453699	0.352683
6	0.919676	0.305050	0.462889	0.352426
8	0.919664	0.305088	0.462765	0.352481
10	0.919671	0.305095	0.462749	0.352493
12	0.919675	0.305096	0.462747	0.352496
14	0.919677	0.305097	0.462747	0.352496

Table 7. Comparison with the SIF between the circular-arc and the oblique edge crack ($F_{I,II} = K_{I,II}/\sigma^{\infty}\sqrt{\pi b}, b = \rho \tan \alpha$)

α	Present analysis		Straight			
	F_I	F_{II}	F_{Is}	F_{IIs}	F_I/F_{Is}	F_{II}/F_{IIs}
15.0	1.0684	0.1720	1.0686	0.1738	0.9998	0.9896
30.0	0.9197	0.3051	0.9201	0.3058	0.9996	0.9977
45.0	0.7044	0.3699	0.7049	0.3645	0.9993	1.0148
60.0	0.4627	0.3525	0.4625	0.3362	1.0004	1.0485
75.0	0.2345	0.2540	0.2318	0.2261	1.0112	1.1234

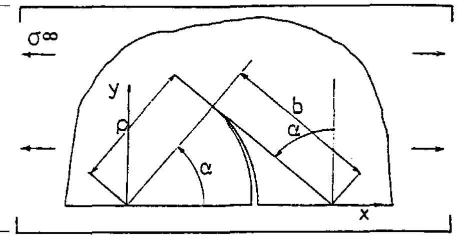

Table 8. Dimensionless SIF of an edge crack that consists of a straight part and circular-arc part ($F_{I,II} = K_{I,II}/\sigma^{\infty}\sqrt{\pi b}, b = c_1 \cos \alpha$)

α	15.0		30.0		45.0		60.0	
c_2/c_1	F_I	F_{II}	F_I	F_{II}	F_I	F_{II}	F_I	F_{II}
0.1	1.0697	0.1604	0.9240	0.2873	0.7117	0.3541	0.4707	0.3465
0.2	1.0689	0.1649	0.9212	0.2950	0.7065	0.3629	0.4639	0.3539
0.4	1.0685	0.1690	0.9197	0.3015	0.7040	0.3692	0.4613	0.3573
0.6	1.0684	0.1706	0.9196	0.3037	0.7040	0.3704	0.4618	0.3562
0.8	1.0684	0.1715	0.9196	0.3047	0.7042	0.3703	0.4624	0.3543
1.0	1.0684	0.1720	0.9197	0.3051	0.7044	0.3699	0.4627	0.3525
Straight	1.0686	0.1738	0.9201	0.3058	0.7049	0.3645	0.4625	0.3362

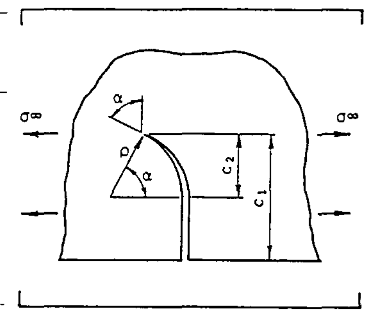

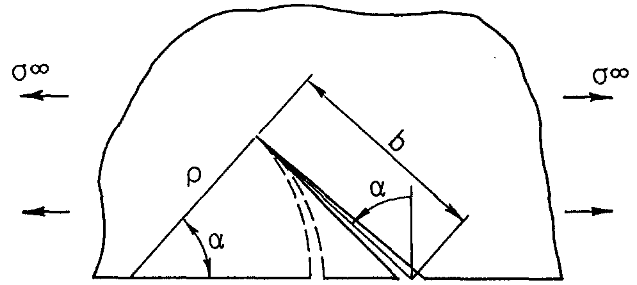

Fig. 5. Oblique edge crack with the same inclination angle at the crack tip and with the same projected crack length.

Table 9. Values of $\hat{F}_I$ of the curved edge crack in a semi-infinite plate under uniform tension, when σ_x on the y-axis is expressed in the form of $\sigma_x = \hat{F}_I \sigma^{\infty} \sqrt{\pi c_1} / \sqrt{2\pi y}$

c_2/c_1 \ α	15.0	30.0	45.0	60.0
0.1	1.124	1.119	1.080	0.984
0.2	1.125	1.122	1.085	0.989
0.4	1.126	1.125	1.090	0.992
0.6	1.126	1.127	1.092	0.991
0.8	1.127	1.128	1.092	0.988
1.0	1.127	1.128	1.092	0.986

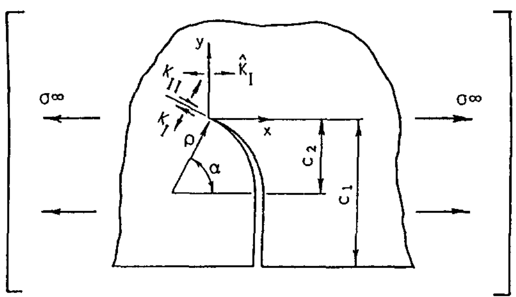

Table 9 shows the values of $\hat{F}_I$. As shown in Table 9, $\hat{F}_I$ is almost constant for $\alpha < 45°$ and is about the same value of straight edge crack, 1.12. Consequently the stress intensity in the direction normal to the tensile axis is nearly equal to that of the straight edge crack with the same projected crack length.

5. Conclusion

In this paper, the method of numerical analysis of the hypersingular integral equation based on the body force method in the curved crack problem was considered. Numerical calculations were carried out for curved cracks under various geometrical conditions, and the effect of curvature at the crack tip on the stress intensity factor was discussed. The conclusions are summarized as follows:

1. Since the convenient formula using Chebyshev polynomial useful for straight crack problems cannot be applied to curved crack problems, in the present numerical method, the unknown

functions are approximated by the product of the fundamental density function and power series. It was found that the present method gives good convergency of the numerical results; in particular, the present result of the circular-arc crack in an infinite plate under uniform tension coincided with the exact solution in the 7 digits.

2. The curved crack that consists of a straight part and a circular-arc part was considered as a basic crack model. Dimensionless SIFs at the curved crack tip B for various values of the relative radius of curvature $\rho/2c$ and the angle α were shown (see Fig. 3). The present results were compared with the SIF of the straight crack with the same inclination angle and with the same projected length. The mode I SIF of an arbitrary curved crack can be approximately given by that of the straight crack with the same inclination angle and with the same projected length of the curved crack, when $\rho/2c > 0.4$ and $\alpha < 45°$. On the other hand, the difference of the values of F_{II} between the curved and the straight crack is quite large.
3. The edge crack that consists of a straight part and a circular-arc part was considered. The dimensionless SIFs for the curved edge crack were shown in comparison with the SIFs for an oblique edge crack. In the case of the edge crack, it was found that the curvature of the crack tip did not have much effect on the stress intensity factor. Hence, the SIF for arbitrary curved edge crack can be evaluated by that of the straight edge crack with the same inclined angle and the projected length of the curved crack.

Acknowledgments

The authors wish to thank Kazumitsu Ishii for his assistance in programing some problems.

References

1. G.C. Sih, P.C. Paris and F. Erdogan, *Transactions of the ASME, Journal of Applied Mechanics* 29 (1962) 306–312.
2. N.I. Muskhelishvili, *Some Basic Problems of the Mathematical Theory of Elasticity*, Noordhoff (1953) 542–545.
3. S.N. Atluri, A.S. Kobayashi and M. Nakagaki, *International Journal of Fracture* 11 (1975) 257–271.
4. B. Cotterell and J.R. Rice, *International Journal of Fracture* 16 (1980) 155–169.
5. N.I. Ioakimidis and P.S. Theocaris, *International Journal of Fracture* 15 (1979) 299–309.
6. Y.Z. Chen, D. Gross and Y.J. Huang, *Engineering Fracture Mechanics* 39 (1991) 791–797.
7. Y. Sumi, S. Nemat-Nasser and L.M. Keer, *International Journal of Fracture* 21 (1983) 67–79.
8. P.S. Leevers, J.C. Radon and L.E. Culver, *Journal of the Mechanics and Physics of Solids* 24 (1976) 381–395.
9. G. Alpa, E. Bozzo and L. Gambarotta, *Engineering Fracture Mechanics* 13 (1980) 791–799.
10. N.A. Noda, H. Umeki and F. Erdogan, *Transactions of the Japan Society of Mechanical Engineers* 55A (1989) 2521–2526.
11. N.A. Noda and K. Oda, *International Journal of Fracture* 58 (1992) 285–304.
12. A.C. Kaya and F. Erdogan, *Quarterly of Applied Mathematics* 45 (1987) 105–122.
13. H.F. Nied, *Transactions of the ASME, Journal of Applied Mechanics* 54 (1987) 642–648.
14. J. Hadamard, *Lectures on Cauchy's Problem in Linear Partial Differential Equations*, Yale University Press (1923).
15. H. Nisitani, *Journal of the Japan Society of Mechanical Engineers* 70 (1967) 627–635. [*Bulletin Japan Society of Mechanical Engineers* 11 (1968) 14–23.]
16. H. Nisitani, D.H. Chen and M. Isida, *Transactions of the Japan Society of Mechanical Engineers* 50 (1984) 341–350.